AN ADVANCED AND IMPROVED ARTIFICIAL NEURAL NETWORK FOR THE PREDICTION OF WAVE OVERTOPPING

Barbara Zanuttigh[1], Sara Mizar Formentin[2], Jentsje W. Van der Meer[3], [4]

This paper focuses on new methods that have been implemented and tested in the Artificial Neural Network (ANN) recently developed by the authors to predict the wave overtopping discharge. An improved representation of the non-significant wave overtopping conditions can be obtained by extending the training database of the existing ANN to include all the non-zero values. The modification of the ANN architecture by the set-up of a classifier-quantifier scheme to improve the prediction of both low and high values of the overtopping is also investigated and discussed. The accuracy of the improved ANN is finally verified through the prediction of new datasets.

INTRODUCTION

The modeling of wave-structure interaction by means of ANNs turned out to be a worthwhile tool in coastal engineering (EurOtop, 2007), in case of complicated structure geometries under a variety of wave conditions. Specific ANNs were developed for the estimation of the wave overtopping discharge q (Van Gent et al., 2007; Verhaeghe et al., 2008), of the wave transmission coefficient K_T (Panizzo and Briganti, 2007) and of the wave reflection coefficient K_R (Zanuttigh et al., 2013).

A new ANN tool has been recently developed by the authors (Zanuttigh et al., 2014) to predict with the same ANN architecture these three parameters, i.e. q, K_T and K_R. It is based on 15 non-dimensional input parameters, of which 4 are related to the wave attack (wave steepness, wave obliquity, shoaling, wave breaking), 9 to the structure geometry (off-shore slopes, width and height of the structure toe, berm, crest) and 2 to the structure characteristics (roughness factor, armour size). The ANN has been trained on an extended version of the CLASH database that is here described as for the wave overtopping data only.

This paper aims at proposing and testing a few modifications that have been implemented in this ANN in order to improve the prediction of q in both cases of significant and non-significant overtopping. Two are the specific objectives of such modifications: the prediction of the low values of q without a systematic overestimation (Van Gent et al., 2007; Zanuttigh et al., 2014) by means of an extension of the ANN training database; the improvement of the accuracy of the predictions by means of a change of the ANN architecture, through a "classifier-quantifiers" scheme (following the previous work by Verhaeghe et al., 2008).

THE WAVE OVERTOPPING DATABASE

The advanced ANN here presented was trained on the database gathered by Zanuttigh et al. (2014), consisting of a total amount of 16'165 tests on wave overtopping, reflection and transmission. This database builds on the CLASH database and adopts the same parameters to schematize the structures geometry and to characterize the wave attack conditions, already identified within the CLASH

[1]Università di Bologna, DICAM, Viale Risorgimento 2, 40136 Bologna, Italy, barbara.zanuttigh@unibo.it
[2]Università di Bologna, DICAM, Viale Risorgimento 2, 40136 Bologna, Italy, saramizar.formentin2@unibo.it
[3]Van der Meer Consulting bv, P.O. Box 11, Akkrum, 8490 AA, The Netherlands, jm@vandermeerconsulting.nl
[4]UNESCO IHE, Westvest 7, Delft, 2611 AX, The Netherlands, j.vandermeer@unesco-ihe.org

project (Van der Meer et al., 2009). In addition to the original CLASH database, the extended version includes the following parameters:

- the average unit size *D* representative of the structure elements;
- the values of K_r and K_t have been included where available;
- the value of the wave directional spreading, when known.

Overall, the extended database consists of:

- 14 hydraulic parameters, characterizing the wave attack conditions;
- 18 structural parameters, for the as general as possible description of the cross-section of the structures;
- 4 "general" parameters, i.e. the reliability and the complexity factors (respectively, *RF* and *CF*), the identification label of the test and the indication of the armour unit/type.

Figure 1 provides a schematization of the cross-sections and illustrates the main hydraulic and geometrical parameters of the database. A more detailed description can be found in Van der Meer et al. (2009). Table 1 reports the type and the number of the 36 parameters included in the extended database, in comparison to the original CLASH database.

The tests in the database are grouped into 7 sections, labelled progressively from A to G. Such partition aims to identify each test according to the structure type and the wave attack conditions: rock permeable straight slopes (group "A"), rock impermeable straight slopes (group "B"), armour units straight slopes ("C"), smooth and straight slopes ("D"), structures with combined slopes and berms ("E"), seawalls ("F") and oblique wave attacks ("G").

From this extended database, the value of the wave overtopping discharge (*q*) is available for 11'825 tests. More than 10'000 tests were derived from the CLASH database (dikes, rubble mound breakwaters, berm breakwaters, caisson structures and combinations with complicated geometries), while the additional data were collected from Victor (2012), smooth steep slopes; Lykke Andersen (2006), reshaping berm breakwaters, and Oumeraci et al. (2007), vertical walls.

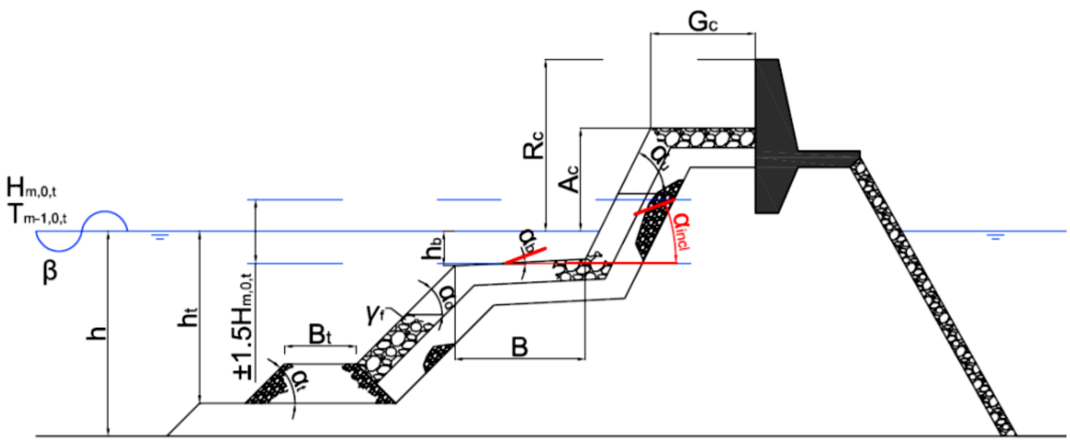

Figure 1. Structure schematization including the hydraulic and structural parameters, based on CLASH.

Table 1. Parameters included in the "new" extended database compared with the ones included in the original CLASH database.

#	Parameter	Unit of measure	Type	CLASH Database	Extended Database
1	*Label*	[-]	general	√	√
2	$H_{m,0,deep}$	[m]	hydraulic	√	√
3	$T_{p,deep}$	[s]	hydraulic	√	√
4	$T_{m,deep}$	[s]	hydraulic	√	√
5	$T_{m-1,deep}$	[s]	hydraulic	√	√
6	h_{deep}	[m]	structural	√	√
7	m	[-]	structural	√	√
8	β	[°]	hydraulic	√	√
9	*Spreading*	[-]	hydraulic		√
10	h	[m]	structural	√	√
11	$H_{m,0,t}$	[m]	hydraulic	√	√
12	$T_{p,t}$	[s]	hydraulic	√	√
13	$T_{m,t}$	[s]	hydraulic	√	√
14	$T_{m-1,t}$	[s]	hydraulic	√	√
15	h_t	[m]	structural	√	√
16	B_t	[m]	structural	√	√
17	γ_f	[-]	structural	√	√
18	$D_{n,50}$	[m]	structural		√
19	*Armour unit*	[-]	general	√	√
20	$cot\alpha_d$	[-]	structural	√	√
21	$cot\alpha_u$	[-]	structural	√	√
22	$cot\alpha_{excl}$	[-]	structural	√	√
23	$cot\alpha_{incl}$	[-]	structural	√	√
24	R_c	[m]	structural	√	√
25	B	[m]	structural	√	√
26	h_b	[m]	structural	√	√
27	$tan\alpha_b$	[-]	structural	√	√
28	B_h	[m]	structural	√	√
29	A_c	[m]	structural	√	√
30	G_c	[m]	structural	√	√
31	*RF*	[-]	general	√	√
32	*CF*	[-]	general	√	√
33	q	[m^3/sm]	hydraulic	√	√
34	*Pow*	[-]	hydraulic	√	√
35	K_r	[-]	hydraulic		√
36	K_t	[-]	hydraulic		√

The assortment of the data included in the overtopping database is described by Figures 2 and 3. Figure 2 shows the distribution of the tests throughout the 7 "sections" from A to G, enhancing that most of the tests belongs to the classes E and F, i.e. refers to impermeable structures (composite dikes and vertical walls) with berms, toe protections and crown walls. Figure 3 characterizes the numerical values of *q*, by grouping the data into 9 classes according to the order of magnitude. The available *q* values range from 10^{-9} to 1 $m^3/s/m$ and a non-negligible portion of data (more than the 11% of the total) are identically equal to 0. The non-zero *q* values are not equally distributed: nearly the 70% of the data falls in the range [10^{-5}; 10^{-3}], while only the 28% is lower than 10^{-5} and less than the 10% is greater than 10^{-3}. As already pointed out by Zanuttigh et. al. (2014), this non-uniform distribution of the experimental data, and in particular the shortage of very high and low values of *q*, is supposed to reduce the ANN capability to represent the "extreme" overtopping rates.

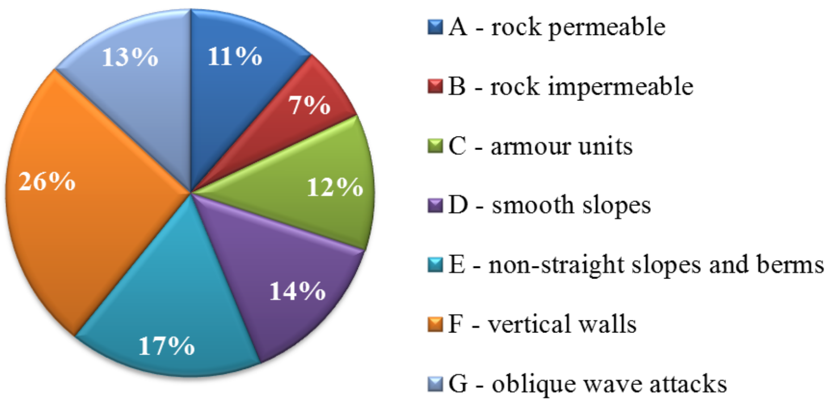

Figure 1. Distribution of the wave overtopping data depending on the structure type within the database.

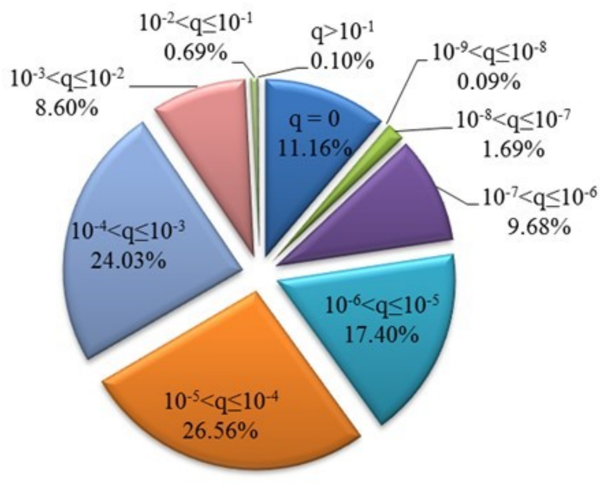

Figure 3. Distribution of the experimental values of *q*, divided into different classes according to the order of magnitude.

THE FEATURES OF THE EXISTING ARTIFICIAL NEURAL NETWORK

An ANN consists of a "black-box" fitting model, which elaborates experimental input and output data, by "learning" the cause-effect relationships between them while completely disregarding the nature of the physical process. The construction of an ANN starts with the identification of the governing parameters (i.e. the *input parameters*) of the process/quantity to be modeled/predicted (i.e. the *output layer*). During the *training* process, the experimental values of the input and output parameters are supplied to the ANN, which "learns" the input-output relationship through the minimization of a selected cost function measuring the error between experimental and predicted values. At the end of the *training*, the ANN is ready to provide estimates of the output parameter for new input conditions. More details can be found in Formentin and Zanuttigh (2013) and Zanuttigh et al. (2014).

The ANN architecture (see Zanuttigh et al., 2014) is characterized by the following features:

- multilayer network, based on a "feed-forward back-propagation" learning algorithm;
- 15 dimensionless input parameters, listed in Tab. 2 in comparison with the 15 dimensional parameters of the ANN developed within the CLASH project (Van Gent et al., 2007);
- 1 hidden layer only; it consists of 40 hidden neurons; this number has been defined after a specific sensitivity analysis;
- 1 output parameter that can be alternatively K_r, K_t and q;
- training algorithm: Levenberg – Marquardt (Levenberg, 1994; Marquardt, 1963);
- hidden neurons transfer function: hyperbolic tangent sigmoid function;
- output neuron transfer function: linear transfer function;
- generalisation technique: bootstrap resampling of the database (see Zanuttigh et al., 2013).

Table 2. Input parameters of the existing ANN (Zanuttigh et al., 2014) and of the ANN developed within the CLASH project (Van Gent et al., 2007).

#	ANN (Zanuttigh et al., 2014)	CLASH ANN (Van Gent et al., 2007)
1	$H_{m,0,t}/L_{m-1,0,t}$	$H_{m,0,t}$
2	$D/H_{m,0,t}$	$T_{m-1,t}$
3	γ_f	γ_f
4	$cot\alpha_d$	$cot\alpha_d$
5	$cot\alpha_{incl}$	$cot\alpha_u$
6	$B/L_{m-1,0,t}$	B
7	$B_t/L_{m-1,0,t}$	B_t
8	$h/L_{m-1,0,t}$	h
9	$h_t/L_{m-1,0,t}$	h_t
10	$h_b/H_{m,0,t}$	h_b
11	$R_c/H_{m,0,t}$	R_c
12	$A_c/H_{m,0,t}$	A_c
13	$G_c/L_{m-1,0,t}$	G_c
14	m	$tan\alpha_B$
15	β	β

THE PREDICTION OF LOW OVERTOPPING DISCHARGES

Both the existing ANNs for the prediction of the wave overtopping developed by Van Gent et al. (2007) and by Zanuttigh et al. (2014) do systematically overestimate the low values of q (q<10^{-5} $m^3/s/m$), presumably because of discarding the values of q<10^{-6} $m^3/s/m$ from the training process. This choice was made following the hypothesis that these low overtopping data are likely to be affected by greater measurement errors (Van Gent et al., 2007). The deterministic value $q=10^{-6}$ $m^3/s/m$ was indeed identified (Verhaeghe et al., 2008) as a threshold value to distinguish between "negligible" and "significant" overtopping, i.e., q<10^{-6} and $q \geq 10^{-6}$ $m^3/s/m$ respectively.

To minimize this overestimation bias, the training database was modified by including all the non-zero values of q, with an increase of the number of the available tests from 6'629 up to 7'577 tests (i.e. 948 additional tests, representing more than the 10% of the total amount of data, see Fig. 3). It is worthy to remark that all the tests characterized by the factors *RF* or *CF* equal to 4 were eliminated from the training, following CLASH (2004).

Table 3 presents the quantitative results of the newly trained ANN in comparison with the original ANN (Zanuttigh et al., 2014). The results are provided in terms of the root mean square error (*rmse*), the Willmott Index (*WI*), the coefficient of determination R^2, as in the previous works by the authors (Formentin and Zanuttigh, 2013; Zanuttigh et al., 2014). The numerical values reported in Tab. 3 are the average indexes and the corresponding standard deviations throughout 100 bootstrapped resamples of the database (Zanuttigh et al., 2014). Tab. 3 reports also the value of the "large errors", which are defined as the percentage of tests (with respect to the total number of tests) for which the ANN gives systematically (i.e., in more than the 50% of the predictions) an output value that differs more than 1.5 times from the experimental corresponding value.

Table 3. Quantitative performance of the newly trained ANN in comparison to the existing ANN by Zanuttigh et al. (2014). The new training database was extended to include all the non-zero values of q.

Prediction of q>0 (# 7'577)				
Training database	RMSE	WI	R^2	Large errors
q>0 (#7'577)	0.040± 0.004	0.986± 0.005	0.95± 0.02	1.8%
Prediction of $q \geq 10^{-6}$ (# 6'629)				
Training database	RMSE	WI	R^2	Large errors
$q \geq 10^{-6}$ (#6'629)	0.046 ± 0.008	0.98 ± 0.01	0.92 ± 0.05	3.8%
q>0 (#7'577)	0.039± 0.005	0.983 ± 0.005	0.95 ± 0.03	0.3%

The extension of the training database leads to a significant improvement of the ANN performance (see the values of *rmse*, R^2 and the percentage of large errors), both when the ANN is used to predict the whole database and only the data with $q \geq 10^{-6}$. The values of *WI* instead are almost equal to the ANN trained on $q \geq 10^{-6}$ only.

Overall it can be also appreciated the reduction of the standard deviation for all the indices, in accordance with the reduction of the large errors.

The qualitative results of the new ANN are provided by Figure 4, showing the distribution of the predicted values q_{ANN} versus the corresponding measurements q_S. By comparing this Figure with Fig. 5 from Zanuttigh et al. (2014), a sensible decrease of the overestimation of q in the range [10^{-6};10^{-5}] $m^3/s/m$ is detected. Moreover, the predictions of the ANN trained on q_s>0 are far more symmetric and less scattered than the original ones with the ANN trained on $q_s \geq 10^{-6}$ $m^3/s/m$ only. The error bands representing the 95% confidence interval are narrower, revealing that the predictions obtained training the ANN on the values of q_s>0 is not only less biased, but also more accurate.

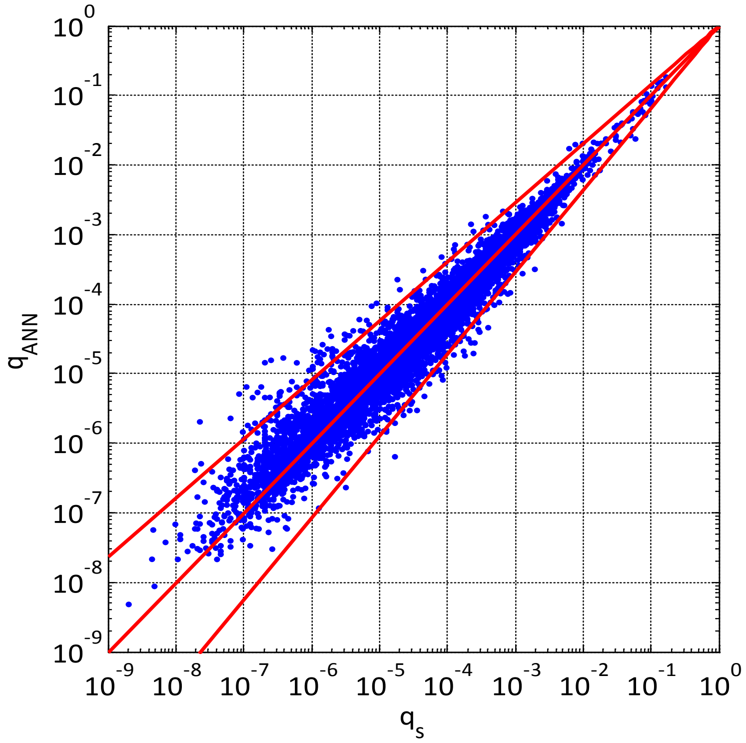

Figure 4. ANN predictions vs experimental values of *q*. All the non-zero values of *q* are included both in training and in prediction.

THE CLASSIFIER-QUANTIFIERS SCHEME

The use of a classifier-quantifier means that the solution is reached into two steps. A first ANN (i.e. "the classifier") provides the preliminary prediction of the data and then the data are either discarded or predicted again by another ANN (i.e. "the quantifier"). In the approach proposed by Verhaeghe et al. (2008), the goal was to identify and discard from prediction the values of $q<10^{-6}$ $m^3/s/m$. The classifier consisted of an ANN trained on the complete CLASH database providing a logical value equal to 0 in case of $q<10^{-6}$ $m^3/s/m$ and 1 otherwise. Only when the logical value was different from 0, the data were quantitatively predicted by the ANN (trained on $q \geq 10^{-6}$ $m^3/s/m$).

The scheme here proposed is rather novel and consists of a quantitative classifier and three quantifiers as it is synthesised in Tab. 4. The classifier is the ANN trained on the extended database (q>0), and it is used to provide a quantitative value of q. Based on this first prediction, the case is then processed by one of the quantifiers, which share the same ANN architecture but are specifically trained on different datasets representing high, average and low values of q.

Figure 5 combines the results of the three ANNs (the quantifiers) showing the overall performance of the classifier-quantifiers against the total database. Tab . 5 reports the error indicators. The main improvement occurs for $q \geq 10^{-3}$, especially in terms of R^2 and WI. As for the remaining two datasets, there is no significant difference between the simple ANN architecture and the classifier-quantifiers scheme. In particular, when predicting the intermediate dataset ($10^{-6}<q<10^{-3}$) the performance is the same, as it would have been expected since the quantifier ANN for this dataset corresponds to the classifier, i.e. the original ANN.

The use of more than one ANN raises the issue whether a continuous prediction is obtained. To this purpose, Figure 6 compares the predictions derived from the newly trained ANN (i.e. the classifier) and from the classifier-quantifiers. The analysis is built up on an existing experiment with varying only the relative crest freeboard R_c/H_{m0t}, by keeping constant all the other geometrical and hydraulic conditions. The discontinuity of the prediction is non-negligible, as it is only one order of magnitude lower than the predicted value.

Table 4. Scheme of the classifier-quantifiers scheme with indication a) of the range of the values of q used for training each classifier and b) of the threshold values of q used to select the quantifiers.

ANN	Training dataset	Threshold values for prediction
Classifier	$q>0$	-
Upper quantifier	$q \geq 10^{-4}$	$q \geq 10^{-3}$
Intermediate quantifier	$q>0$	-
Lower quantifier	$0 \leq q \leq 10^{-5}$	$q \leq 10^{-7}$

Table 5. Quantitative performance of the classifier-quantifier scheme.

Predicting database	RMSE	WI	R^2	Large errors
q>0 (#7‘577)	0.045 ± 0.006	0.978± 0.01	0.92± 0.04	4.4%
$q \geq 10^{-3}$ (#785)	0.033± 0.009	0.975± 0.02	0.91± 0.09	0.0%
$10^{-3} \leq q \leq 10^{-6}$ (#6‘532)	0.045± 0.005	0.977± 0.009	0.91± 0.02	0.8%
$q \leq 10^{-6}$ (#260)	0.085± 0.05	0.83± 0.1	0.6 ± 0.1	18%

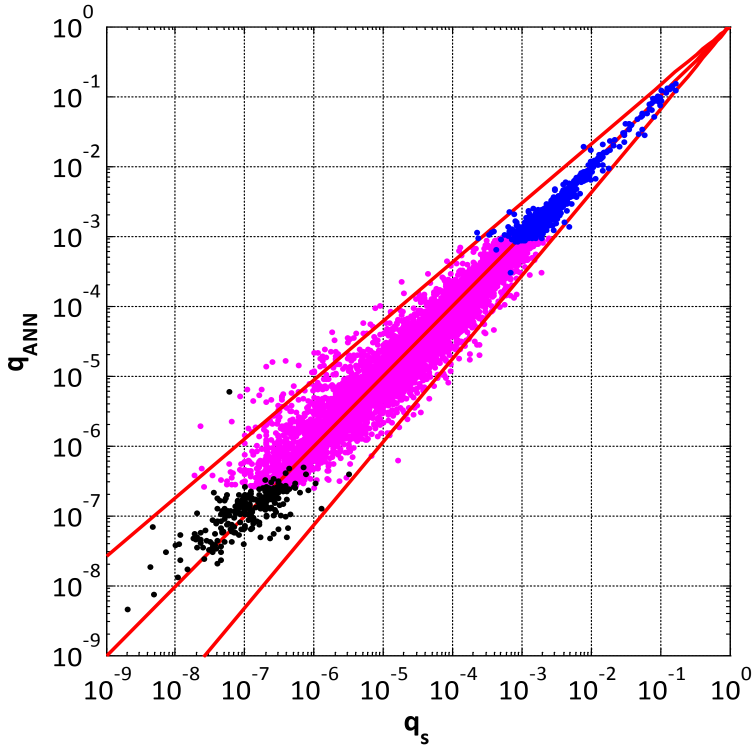

Figure 5. Performance of the classifier-quantifiers predicting the whole database. The coloured points highlight the predictions by the quantifiers.

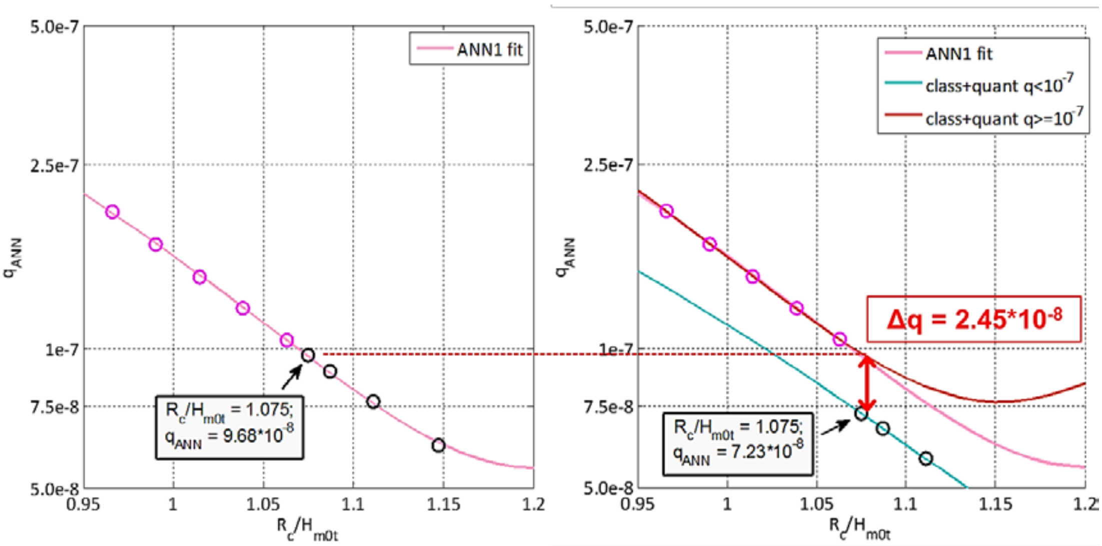

Figure 6. Variation of the predicted discharge q_{ANN} as a function of R_c/H_{m0t}, keeping constant all the other geometrical and hydraulic conditions. Results from the classifier only to the left, from the classifier-quantifiers to the right. The right plot shows the zoomed view around R_c/H_{m0t}=0.64, i.e. at the boundary between the intermediate and the lower quantifiers (q=10^{-7}).

THE PREDICTION OF NEW DATASETS

The accuracy of the newly trained ANN was tested against the prediction of new data, i.e. data not included yet in the training database. For this purpose, the following two datasets were considered:

- 56 tests on rubble mound with cobs (Besley et al., 1993);
- 103 tests on harbour caissons (private communication), with and without berms, and characterized by different revetment blocks (tetrapods, antifers, core-locs).

The ANN predictions of these two datasets are respectively shown in Figures 7 and 8 in comparison to the corresponding measurements. Both the plots report also the prediction of the whole database and the related confidence bands.

The rubble mound with cobs dataset (Fig. 7) is very well represented by the ANN, as nearly all the predicted values fall within the confidence bands.

A slight tendency of overestimating the tests on caissons is instead observed from Fig. 8. This can be explained by considering that the training database includes only 44 tests on caissons, 30 tests on circular caissons and 13 tests on caissons with an accropod berm (all from private communication). Indeed, all these tests are characterized by values of γ_f ranging from 0.7 to 1, while the presence of the revetment blocks in the new dataset of caissons determines lower values of γ_f, which is on average equal to 0.45-0.50. Nevertheless, the ANN predictions are still good, since the number of the outliers is rather limited in number (representing approximately the 25% of the whole dataset).

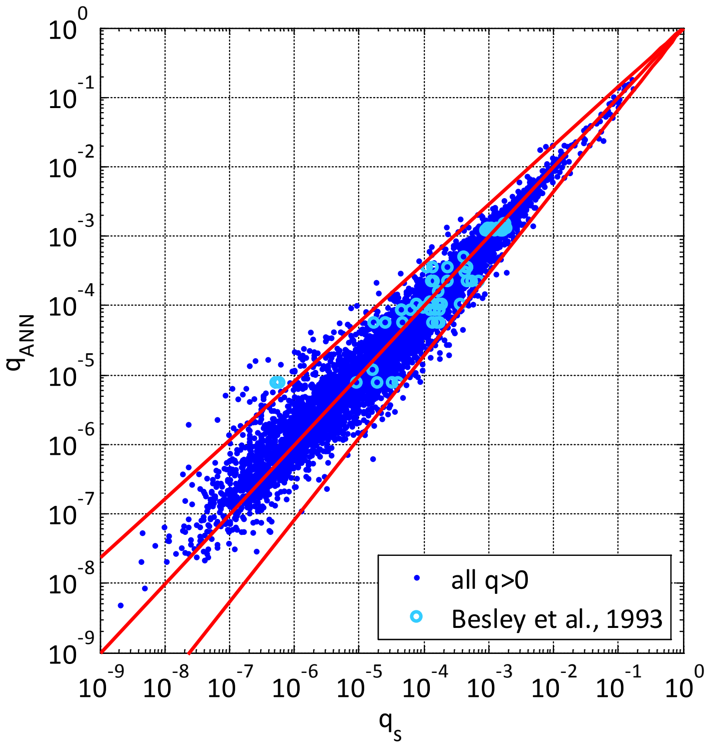

Figure 7. Predictions q_{ANN} versus the experimental values q_s in case of the new dataset of rubble mound with cobs from Besley et al. (1993).

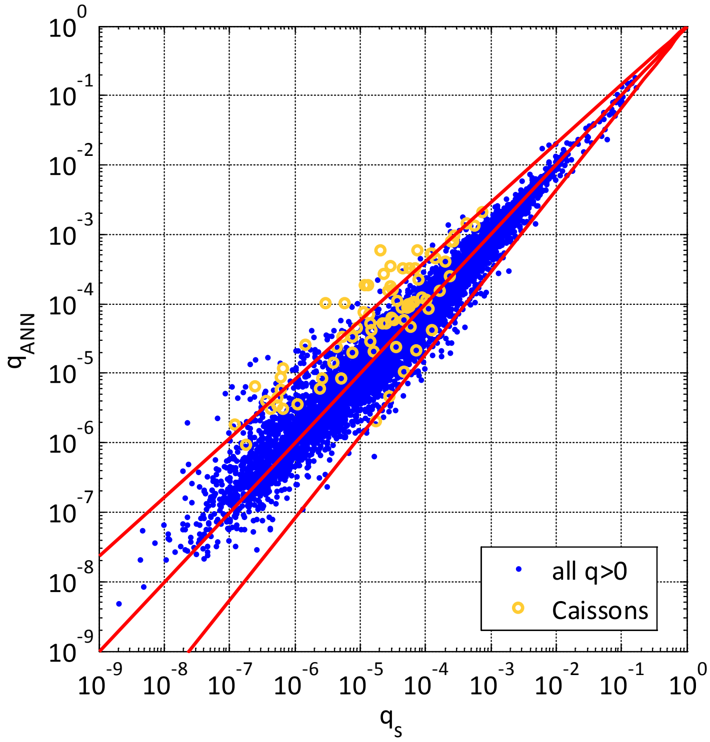

Figure 8. Predictions q_{ANN} versus the experimental values q_s in case of the new dataset of harbour caissons.

CONCLUSIONS

This paper presented a few methodological changes implemented in the existing ANN recently developed by the authors (Zanuttigh et al., 2014) to predict the overtopping discharge *q* for differnet structure geometries under a variety of wave conditions. The ANN consists of a multi-layer network, with 15 non-dimensional input parameters, 40 hidden neurons and 1 output parameter, i.e. the average overtopping discharge *q*.

Differently from previous works (Van Gent et al., 2007; Verhaeghe et al., 2008; Zanuttigh et al., 2014), the ANN has been here trained on the extended database set-up by the authors by including all the laboratory-scale non-zero values of *q*. It has been shown that this choice allows to significantly reduce the bias of the ANN predictions in case of low values of *q*, i.e. the systematic overestimation that occurred for $q<10^{-6}$ $m^3/s/m$. The results of the newly trained ANN are satisfactorily accurate, being the average values of the *rmse*, *IW* and R^2 indices respectively equal to 0.040, 0.985 and 0.95, in comparison with the values 0.046, 0.98 and 0.92 that were respectively derived when using only the values of $q \geq 10^{-6}$ for the training.

Specifically to improve the representation of the extreme values of *q*, a classifier-quantifier scheme was implemented and verified. The scheme consists of a quantitative classifier, which is the ANN trained on the complete database, and three classifiers, which are the same ANN but trained on three datasets representing high, intermediate and low values of *q*. Based on the first prediction from the classifier, the input is processed by one of the three quantifiers, being the final prediction affected by the eventual error propagation from the classifier. While the prediction of the high values of q slightly improves, the overall ANN performance decreases due to a worsening of the prediction of the low values of q, leading to the recommendation to keep the ANN architecture simple, i.e. by using the classifier only.

The accuracy of the optimised ANN has been tested by predicting new datasets. In most of the cases, the predictions fall within the 95% confidence bands and show the same dispersion as the predictions of the training database.

ACKNOWLEDGEMENTS
The support of the European Commission through FP7.2009-1, Contract 244104, THESEUS (www.theseusproject.eu), is gratefully acknowledged.

REFERENCES

Besley P., Reeves M. and Allsop N.W.H., 1993. Random wave physical model tests: overtopping and reflection performance, Report IT 384, HR Wallingford.

CLASH, 2004. Crest Level Assessment of coastal Structures by full scale monitoring, neural network prediction and Hazard analysis on permissible wave overtopping. EVK3-CT-2001-00058. www.clash-eu.org.

EurOtop, 2007. European Manual for the Assessment of Wave Overtopping. T. Pullen, N.W.H. Allsop, T. Bruce, A. Kortenhaus, H. Schüttrumpf and J.W. van der Meer. At: www.overtopping-manual.com.

Formentin, S. M. and Zanuttigh B. 2013. Prediction of wave transmission through a new artificial neural network developed for wave reflection. Proceedings of 7th International Conference on Coastal Dynamics, http://www.coastaldynamics2013.fr/pdf_files/057_Formentin_SaraMizar.pdf.

Lykke Andersen, T. and Burcharth, H.F., 2004. CLASH Work package 4.4 - D24 Report on additional tests. Part D Berm breakwater tests. On-line available.

Panizzo, A., Briganti, R, 2007. Analysis of wave transmission behind low crested breakwaters using neural networks, Coastal Engineering, 54, 643–656.

Van der Meer, J.W., Verhaeghe, H., Steendam, G.J., 2009. The new wave overtopping database for coastal structures. Coastal Engineering 56, 108–120.

Van Gent, M.R.A., van den Boogaard, H.F.P., Pozueta, B. and Medina, J.R. 2007. Neural network modelling of wave overtopping at coastal structures. Coastal Engineering 54, 586–593.

Verhaeghe, H., De Rouck, J., van der Meer, J.W., 2008. Combined classifier–quantifier model: a 2-phases neural model for prediction of wave overtopping at coastal structures. Coastal Engineering 55, 357–374.

Zanuttigh, B., Formentin, S.M. and Briganti, R., 2013. A Neural Network for the prediction of wave reflection from coastal and harbor structures, Coastal Engineering 80, 49-67.

Zanuttigh, B., Formentin, S., & Van der Meer, J. 2014. Advances in modelling wave-structure interaction through artificial neural networks. Coastal Engineering Proceedings, 1(34), structures.69.
doi:http://dx.doi.org/10.9753/icce.v34.structures.69